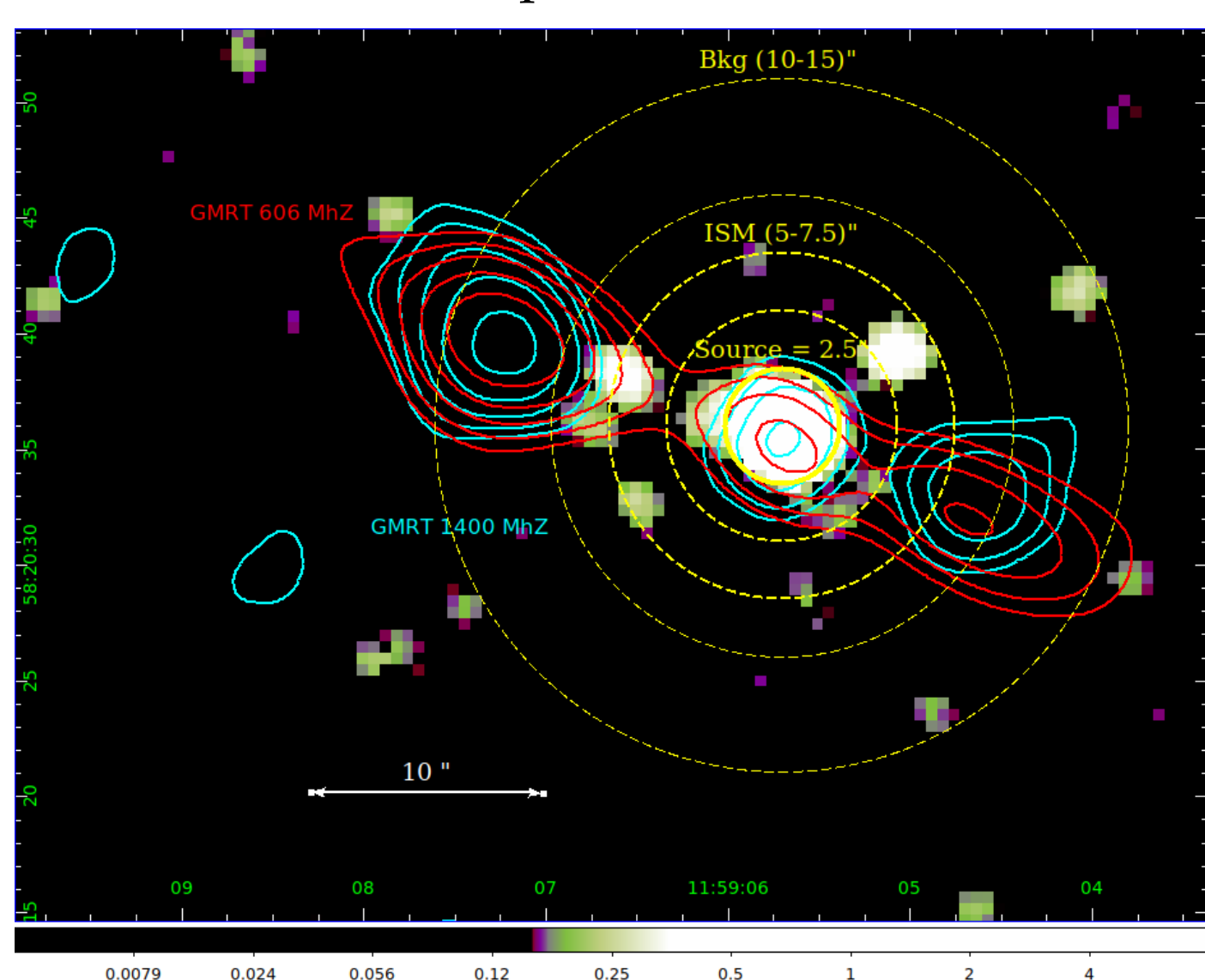


## Introduction

- In Active Galactic Nuclei (AGN), relativistic jets and high-energy emission of accretion disks can interact with the interstellar medium (ISM) of host galaxies by ionizing, heating, mixing, and pushing out the surrounding gas, affecting in this way the properties and structure of the hosts.
- Here we report on the *Chandra* data analysis for the two peculiar radio sources representing different snapshots of the intermittent jet activity in low-power AGN.
- For both targets, we performed detailed PSF simulations that allowed us to investigate the surface brightness profiles of the X-ray emission, and to properly extract the spectra of the unresolved nuclei, gaseous envelopes of host galaxies, and the backgrounds.
- Due to the low photon statistics (several hundreds of counts within the 0.5–7.0 keV range in both cases), thus selected spectra were then modelled (together with the backgrounds) by applying the Poisson likelihood (Cstat), and assuming different emission scenarios (including the absorbed power law, the multi-temperature thermal plasma, etc.).

## CGCG 292-057

- Here we present the final results of the data analysis and modeling of CGCG 292-057 ( $z=0.054$ ), observed by ACIS-S detector, for 93 ksec. It is hosted by a post-merger bulge-dominated galaxy with a LINER type nucleus, and is characterized by a complex radio morphology, consisting of arc-second scale inner lobes extending for about 20 kpc, embedded within the arcmin-scale outer radio halo (Kozieł- Wierzbowska et al. 2012, Singh et al. 2015).
- This system is a particularly interesting example of a post-merger starforming galaxy, with recurrent jet activity: the outer lobes are believed to have formed during the previous, long-terminated cycle of the jet activity, while the inner coaxial lobes are considered as a manifestation of a new episode of the enhanced jet production in the system, triggered by a sudden increase in the central black hole accretion rate.
- It was observed in ACIS-I instrument in cycle 16, with the exposure totalling to 93.8 ksec. The source was placed at the aim point on the back-illuminated ACIS CCD.
- The data were collected in the VFAINT mode and the observation was made in the POINTING mode. The target was detected with the total number of net counts of 385 within 0.5-7.0 keV.
- The X-ray data analysis was performed with the CIAO v.4.11 software using CALDBv.4.8.2. Spectral modeling was done in Sherpa using the Cash and Cstat fitting statistics and the Nelder-Mead & Moncar optimization method.



**Figure 1:** The ACIS-S image of central region in the CGCG 292–057 system, along with the GMRT radio contours. The contour levels are spaced by a factor of  $\sqrt{2}$ , and the first contour is  $0.60 \text{ mJy beam}^{-1}$

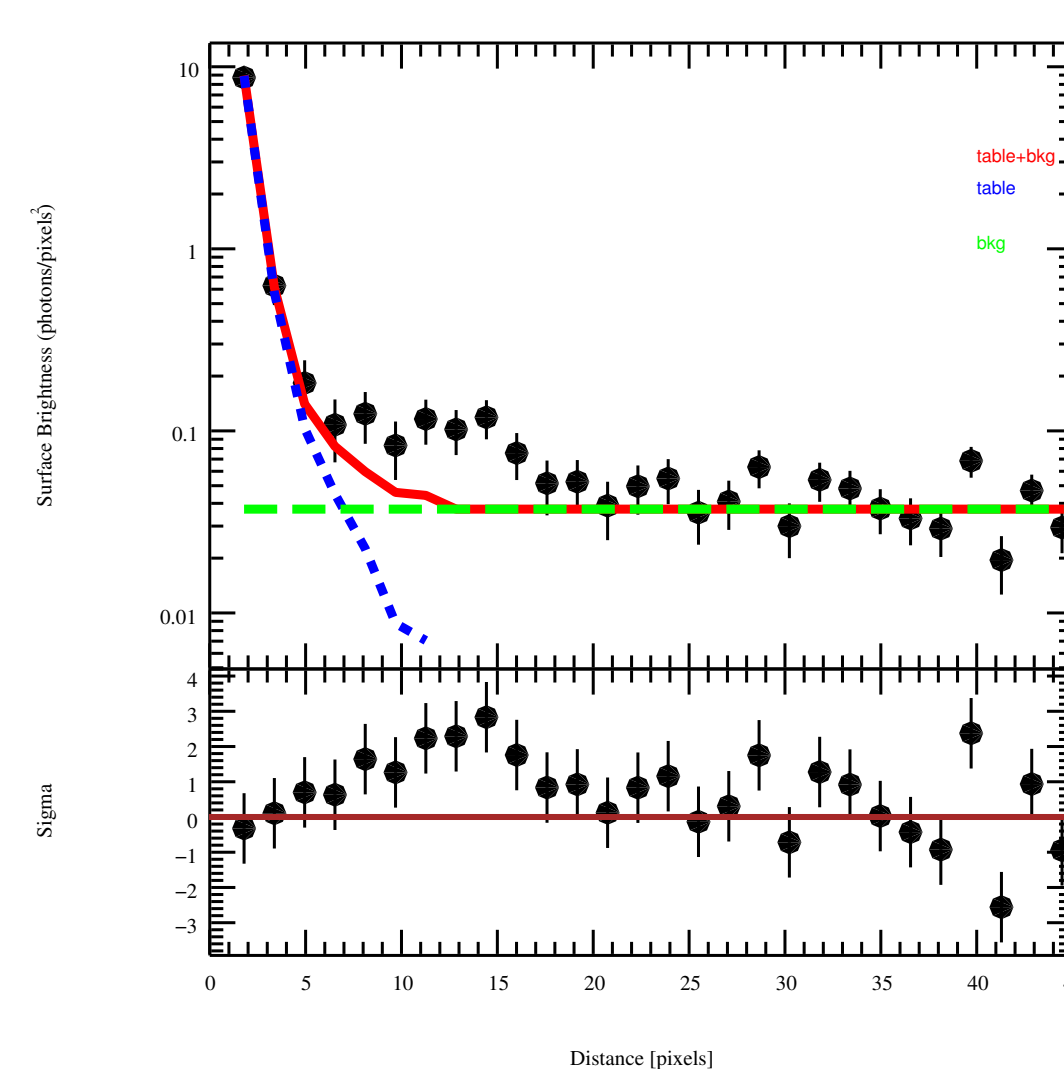


**Figure 2:** X-ray surface brightness profile of CGCG 292–057, along with the fit including the table model for the PSF and a constant background.

**Table 1:** Spectral modeling of the CGCG 292–057 nucleus

Model	$N_{\text{H}}^{(1)}$ [ $\times 10^{22} \text{ cm}^{-2}$ ]	$N_{\text{H}}^{(2)}$ [ $\times 10^{22} \text{ cm}^{-2}$ ]	$kT^{(a)}$ [keV]	$kT^{(b)}$ [keV]	$\Gamma$	$E_{\text{line}}$ [keV]	$EW_{\text{line}}$ [eV]	Cstat/DOF
(1)	(2)	(3)	(4)	(5)	(6)	(7)	(8)	(9)
PL	0.027	—	—	—	$-0.36 \pm 0.041$	—	—	817.1/887
PL+G	0.052	—	—	—	$-0.312 \pm 0.05$	6.759	124.1	815.03/884
Apec	$3.15 \pm 0.36$	—	$> 10$	—	—	—	—	866.629/884
Apec+PL	$1.38 \pm 0.39$	$3.96 \pm 0.964$	$0.12 \pm 0.056$	—	$1.094 \pm 0.35$	—	—	784.31/884
Apec+Apec	$4.61 \pm 0.50$	$1.075 \pm 0.16$	$> 10$	$0.21 \pm 0.015$	—	—	—	783.726/884
Scat. PL+G	$0.092 \pm 0.070$	$6.69 \pm 0.48$	—	—	$1.787 \pm 0.238$	$6.754 \pm 0.023$	320.4	783/884

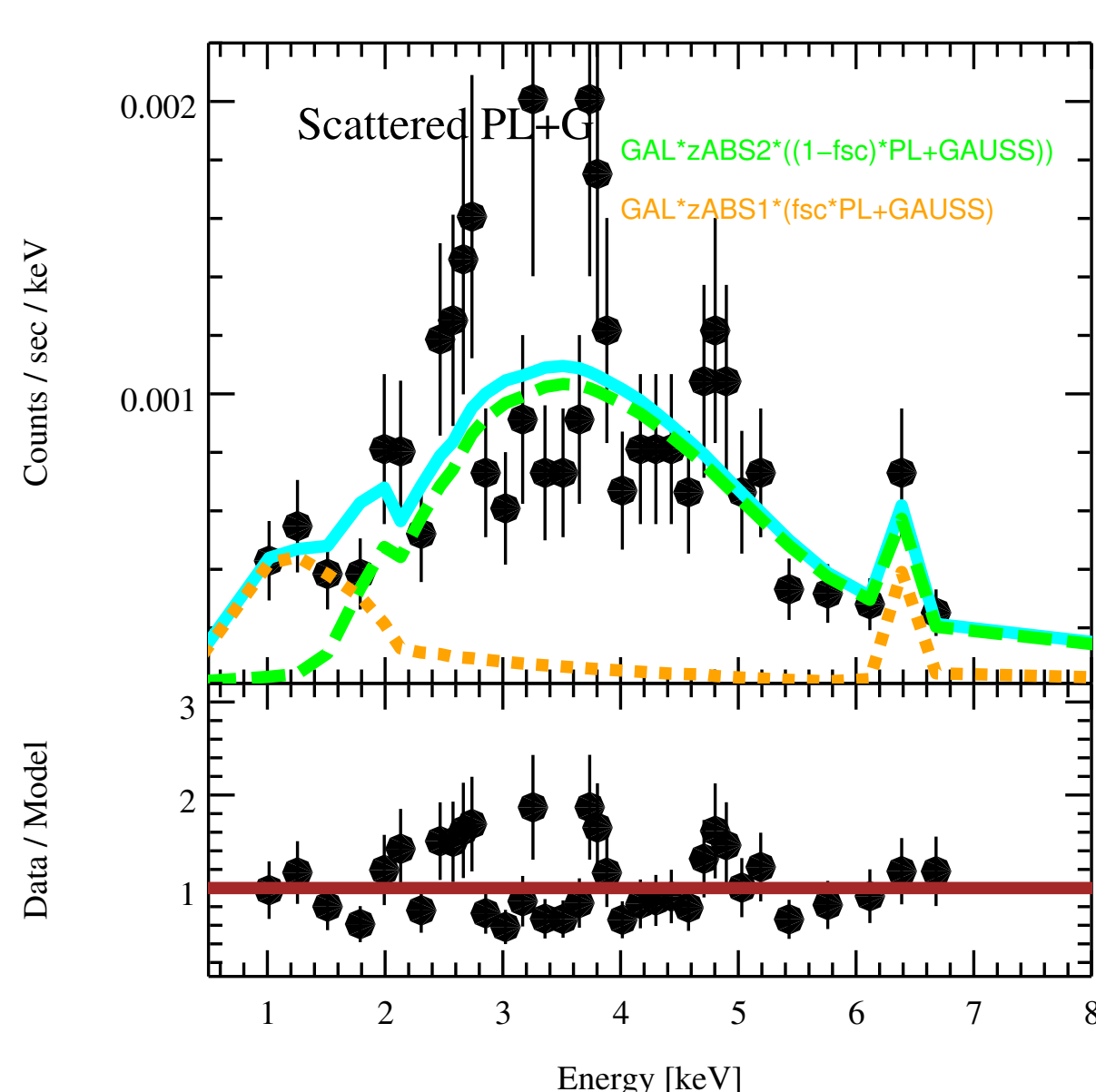


**Figure 3:** *Chandra* spectrum of the CGCG 292–057 nucleus, fitted with the “scattered power-law + gauss” model  $\text{zphabs1} * (1 - \text{fsc}) * \text{PL} + \text{zphabs2} * (\text{fsc} * \text{PL} + \text{xszgass})$ ; scattered fraction  $\text{fsc} = 0.031$ .

**Table 2:** Results of the simultaneous fitting of the ISM (= source) and the BCG (= background) regions.

Region	Model/Parameter	Value/Value with 1 $\sigma$ errors	Unit <sup>†</sup>
BCG	powerlaw		
	$\Gamma_{\text{bcg}}$	$0.87 \pm 0.15$	
ISM	PL ampl	$(8.62 \pm 1.48) \times 10^{-7}$	$\text{ph/keV/cm}^2/\text{s at } 1 \text{ keV}$
	$\text{zphabs} * \text{sapec}$		
	$N_{\text{H}}$	$0.528^{+0.14}_{-0.23}$	$10^{22} \text{ cm}^{-2}$
	$kT_{\text{isa}}$	$0.81^{+0.25}_{-0.25}$	keV
	Norm	$(2.21 \pm 0.65) \times 10^{-6}$	$10^{-14} (1+z)^2 n^2 V / 4\pi d_L^2$
BCG	C-stat./DOF	455.35/887	
	powerlaw		
ISM	$\Gamma_{\text{isc}}$	$0.87 \pm 0.18$	
	PL ampl	$(8.44 \pm 1.64) \times 10^{-7}$	$\text{ph/keV/cm}^2/\text{s at } 1 \text{ keV}$
	$\text{zphabs} * \text{powerlaw}$		
	$N_{\text{H}}$	$0.318^{+0.05}_{-0.05}$	$10^{22} \text{ cm}^{-2}$
	$\Gamma_{\text{isc}}$	$4.01 \pm 1.78$	
ISM	PL ampl	$(1.87 \pm 1.86) \times 10^{-7}$	$\text{ph/keV/cm}^2/\text{s at } 1 \text{ keV}$
	C-stat./DOF	455.28/887	

## Conclusions

- In both systems we have detected the fluorescence iron lines; in CGCG 292-057 the line is from an ionized reflector, and we speculate that the ionized gas responsible for the line production could be identified with dense clouds of the ISM engulfed within the expanding lobes.
- The diffuse excess X-ray emission (over the core PSF and the constant background) is seen on the scale of several/tens of arcsec in both targets; in CGCG 292-057 this excess is seen strictly around the edges of the innermost radio structure ( $\sim \text{kpc}$  distances from the core), and hence

we identify it with the hot diffuse component of the ISM compressed and heated (up to  $\lesssim 1 \text{ keV}$  temperatures) by the expanding jets/lobes; in CGCG 292–033, the excess X-ray emission is consistent with a halo of a hot gas characteristic for an early-type host.

- In the forthcoming papers we discuss in detail the results of the spectral and surface brightness analysis for both targets.

## CGCG 292-033

We present an analogous, although in this case still preliminary analysis of the archival and previous unpublished 40 ksec-long *Chandra* exposure of CGCG 292-033 ( $z=0.01075$ ), observed by ACIS-S detector. It is hosted by an elliptical galaxy in a non-interacting pair, again with the LINER-type nucleus, and possesses an extremely compact, mas-scale double-lobe structure with the projected extent of a few parsecs, indicative of the newly born jets (Taylor et al. 1998).

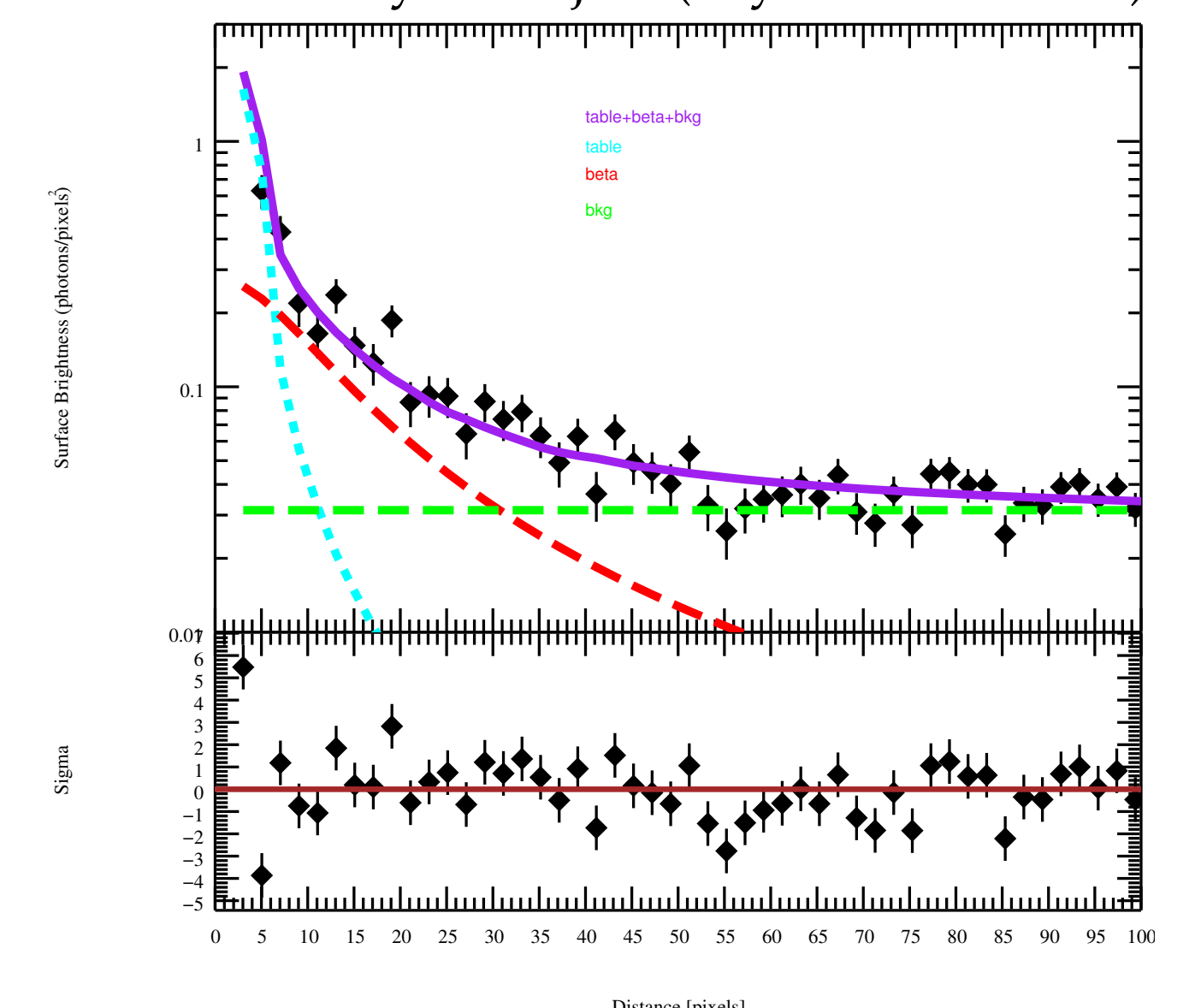
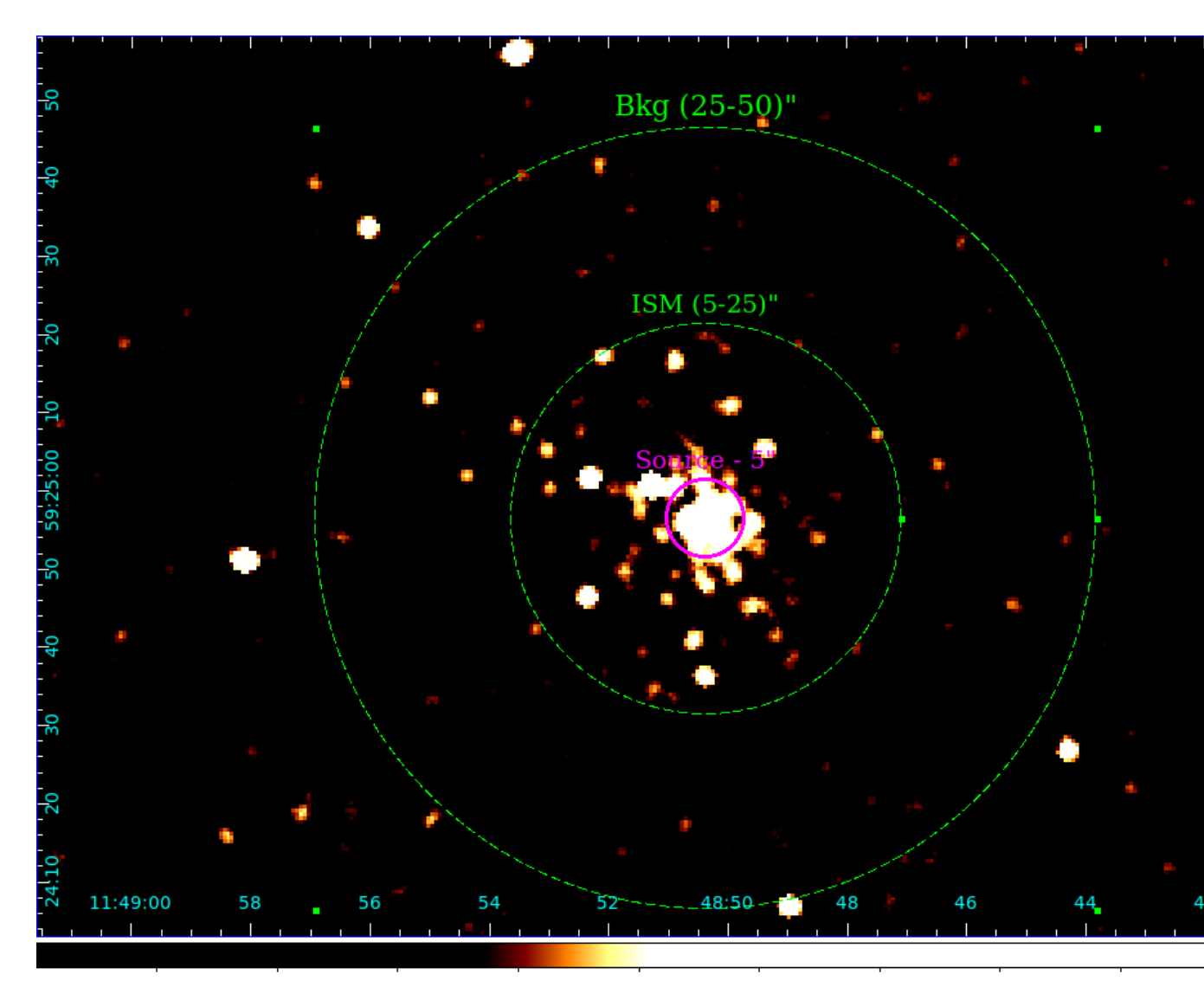


**Figure 4:** The ACIS-S image of CGCG 292–033 system, showing the source, the ISM and the background regions. **Figure 5:** X-ray surface brightness profile of CGCG 292–033 nucleus, along with the fit including the table model for the core PSF, constant background, and the beta model.

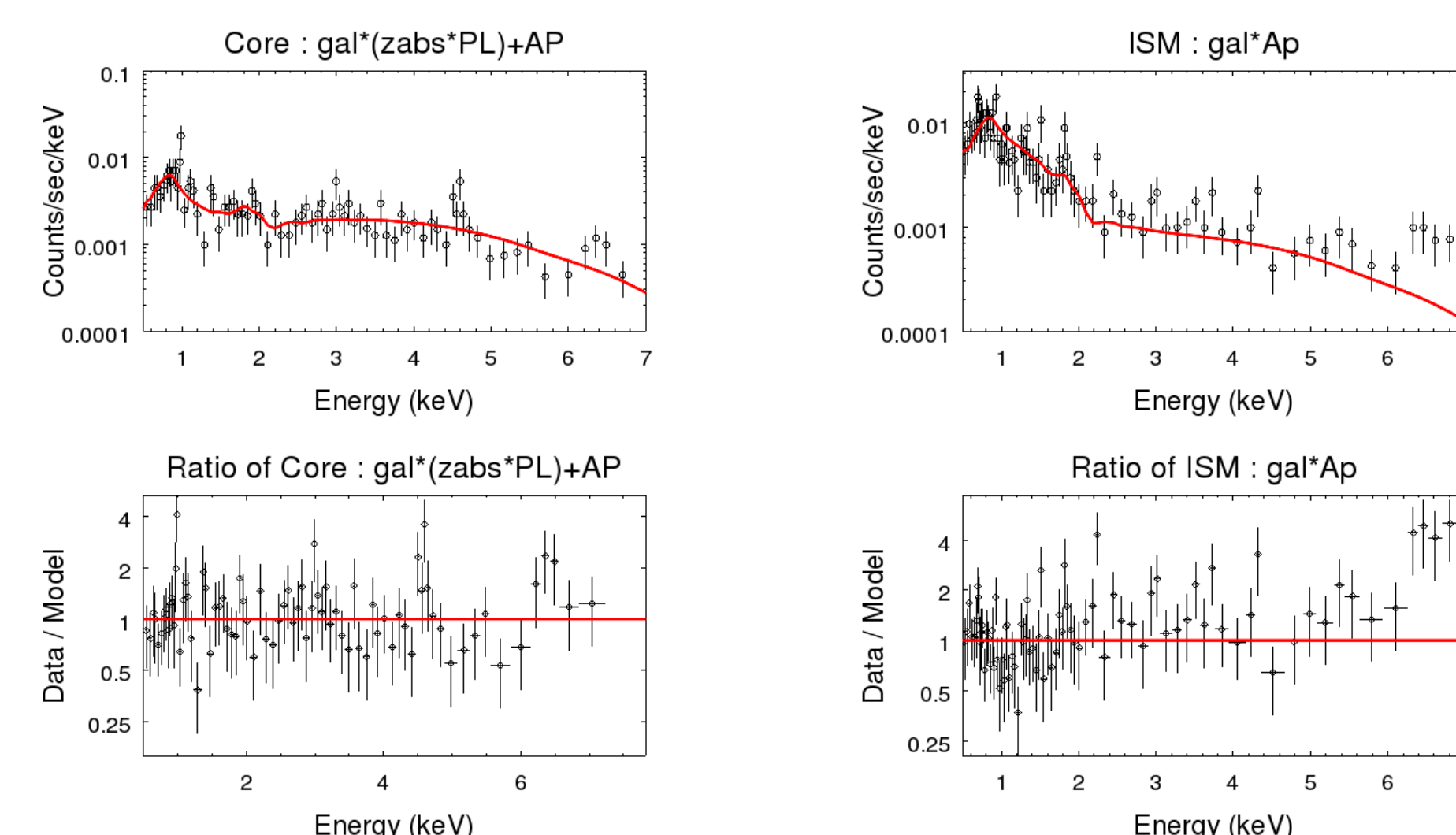


**Figure 6:** *Chandra* spectrum of the CGCG 292–033 nucleus, fitted with the model  $(\text{zphabs1} * \text{PL}) + \text{Apec}$

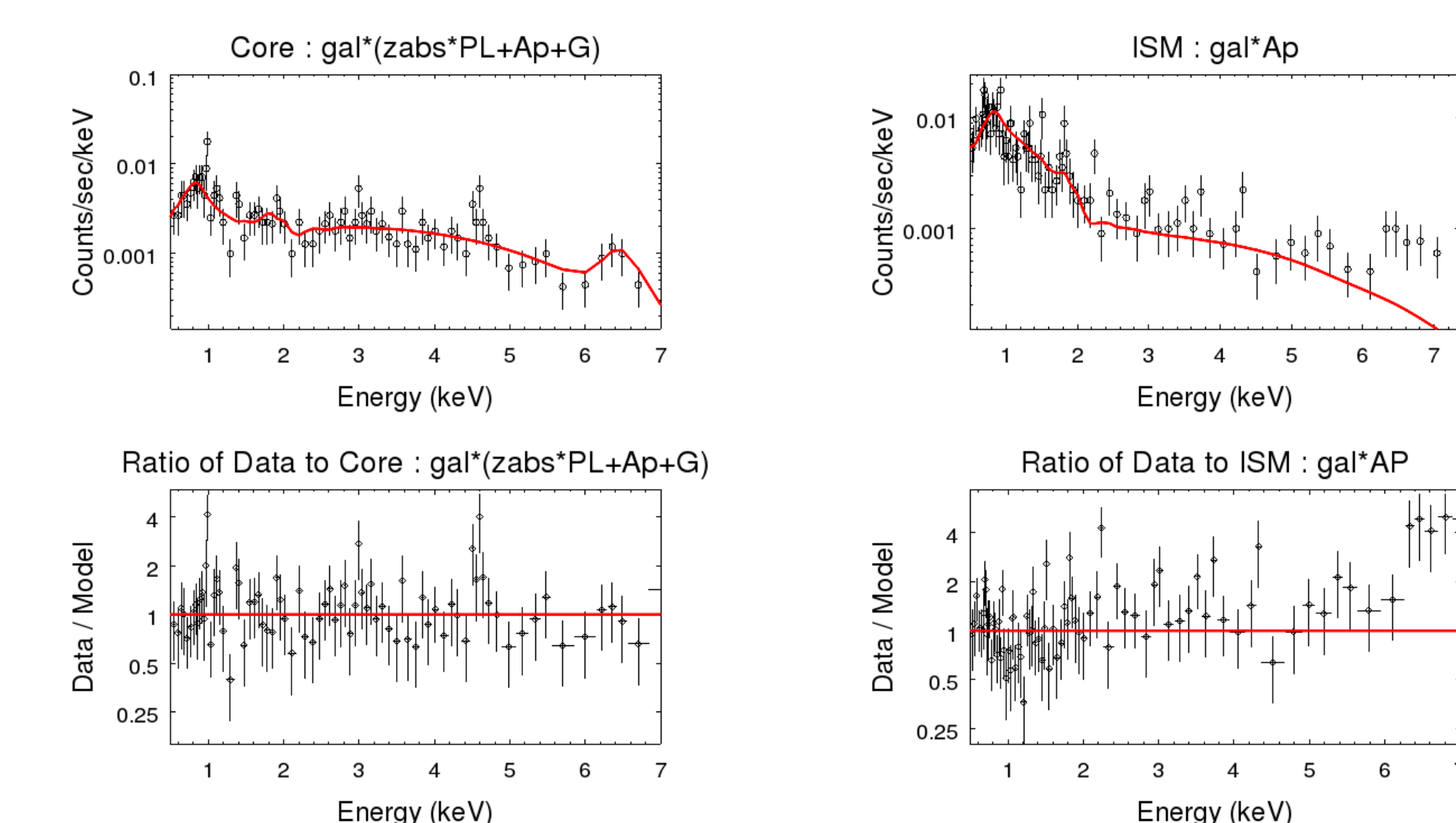


**Figure 7:** *Chandra* spectrum of the CGCG 292–033 nucleus, fitted with the model  $\text{zphabs1} * (\text{PL} + \text{Apec} + \text{Gauss})$ .

**Table 3:** Spectral modelling of the CGCG 292–033 nucleus

Model <sup>src</sup>	$N_{\text{H}}$ [ $\times 10^{22} \text{ cm}^{-2}$ ]	$kT$ [keV]	$E_{\text{line}}$ [keV]	$EW_{\text{line}}$ [keV]	$\Gamma^{\text{src}}$	$\Gamma^{\text{bcg}}$	Cstat/DOF
$\text{zabs} * (\text{PL} + \text{Apec})$	$2.56^{+1.77}_{-1.15}$	$0.76^{+0.16}_{-0.097}$	—	—	$1.06^{+0.80}_{-0.41}$	$0.66^{+0.072}_{-0.081}$	1.41
$\text{zabs} * (\text{PL} + \text{Apec} + \text{Gauss})$	$3.04 \pm 0.74$	$0.76 \pm 0.063$	$6.52^{+0.13}_{-0.12}$	1.033	$1.48 \pm 0.33$	$0.65 \pm 0.041$	1.44

## References

- [1] Kozieł-Wierzbowska, D., et al. 2012, MNRAS, 422, 1546
- [2] Singh, V., et al. 2015, MNRAS, 454, 1556
- [3] Taylor, G. B., et al. 1998, ApJ, 498, 619

## Acknowledgment

This work was supported by the Polish NSC grant 2016/22/E/ST9/00061 (K.B., Ł. S., V.M.) and the *Chandra* guest investigator program GO5-16109X. This research was supported in part by NASA through contract NAS8-03060 (A.S., M.S.) to the *Chandra* X-ray Center.